IMMUNOLOGY

Homeostasis and transitional activation of regulatory T cells require c-Myc

Jordy Saravia[1], Hu Zeng[1]*, Yogesh Dhungana[1], Daniel Bastardo Blanco[1,2], Thanh-Long M. Nguyen[1], Nicole M. Chapman[1], Yanyan Wang[1], Apurva Kanneganti[1], Shaofeng Liu[1], Jana L. Raynor[1], Peter Vogel[3], Geoffrey Neale[4], Peter Carmeliet[5], Hongbo Chi[1†]

Regulatory T cell (T_{reg}) activation and expansion occur during neonatal life and inflammation to establish immunosuppression, yet the mechanisms governing these events are incompletely understood. We report that the transcriptional regulator c-Myc (Myc) controls immune homeostasis through regulation of T_{reg} accumulation and functional activation. Myc activity is enriched in T_{regs} generated during neonatal life and responding to inflammation. Myc-deficient T_{regs} show defects in accumulation and ability to transition to an activated state. Consequently, loss of Myc in T_{regs} results in an early-onset autoimmune disorder accompanied by uncontrolled effector $CD4^+$ and $CD8^+$ T cell responses. Mechanistically, Myc regulates mitochondrial oxidative metabolism but is dispensable for fatty acid oxidation (FAO). Indeed, T_{reg}-specific deletion of Cox10, which promotes oxidative phosphorylation, but not Cpt1a, the rate-limiting enzyme for FAO, results in impaired T_{reg} function and maturation. Thus, Myc coordinates T_{reg} accumulation, transitional activation, and metabolic programming to orchestrate immune homeostasis.

INTRODUCTION

Regulatory T cells (T_{regs}) play a crucial role in immune suppression and inhibition of autoimmunity (*1*). Integral to T_{reg}-mediated maintenance of immune homeostasis during perinatal life and after acute inflammatory insults is the ability to expand in response to proinflammatory stimuli (*2*). This self-regulating, dynamic process is dependent on spatial and temporal signals, which influence proliferation, migration, and suppressive capacity of T_{regs}. It has become clear that T_{regs} are heterogeneous, with respect to the activation state (*2*–*4*). Central T_{reg} cells (cT_{regs}) represent a more quiescent, resting subpopulation, while effector T_{reg} cells (eT_{regs}) share qualities of more activated effector T cell subsets.

We and others have demonstrated that cellular metabolic regulation is interwoven with immune cell function and differentiation (*5*–*8*). Upon activation, T cells transition from quiescence to activation and effector differentiation by shifting from catabolic [i.e., fatty acid oxidation (FAO), autophagy, etc.] to anabolic (i.e., glycolysis, glutaminolysis, etc.) metabolism to generate sufficient energy and biosynthetic materials necessary for rapid proliferation and effector function (*9*). Previous work has shown that this metabolic reprogramming during lymphocyte activation, as well as in rapidly proliferating cancer cells, is dependent on the master transcriptional regulator c-Myc (Myc) (*9*, *10*). This vital role of Myc has been described in conventional $CD4^+$ and $CD8^+$ T cells (*9*). However, the function of Myc in T_{regs}, a metabolically unique subset of T cells (*5*, *7*, *11*, *12*), remains unclear.

We have recently reported that mitochondrial function is indispensable for eT_{reg} generation and function in vivo (*13*). While multiple nutrient inputs can drive mitochondria-dependent oxidative metabolism, the prevailing view is that FAO is a major metabolic pathway for T_{regs} (*14*, *15*) and other quiescent cell types, such as memory T cells (*16*). Moreover, Foxp3 has been shown to promote FAO and oxidative phosphorylation while dampening Myc expression and target gene expression (*17*), as well as PI3K (phosphatidylinositol 3-kinase) and anabolic metabolism (*18*). However, genetic models that target FAO reveal a disposable role of carnitine palmitoyltransferase (Cpt1a, the dominant isoform mediating FAO in immune cells) in T cell responses, unlike the effects observed with the pharmacological inhibitor etomoxir (*19*, *20*). Considering our increasing knowledge on T_{reg} metabolism and functional fitness during activation (*5*, *7*, *11*), T_{reg}-specific roles of FAO and oxidative metabolism warrant further investigation.

Here, we show that Myc is vital for proper T_{reg} function during the early stages of postbirth development and in response to acute inflammation. Myc is abundantly expressed in neonatal T_{regs} undergoing homeostatic expansion, and T_{reg}-specific deletion of *Myc* results in a rapid, fatal autoimmune disorder characterized by systemic inflammation and tissue damage. Myc-deficient T_{regs} exhibit a cell-intrinsic activation defect and are unable to undergo expansion or develop into eT_{regs} in response to induced inflammation in vivo. The functional necessity of Myc in T_{regs} appears to be temporally specific, as we unexpectedly find that eT_{reg} status is unaffected by induced Myc deletion in vivo at steady state. Although Myc is essential for regulating mitochondrial function in T_{regs}, this effect is not linked to changes in FAO. Mice with Cpt1a-deficient T_{regs} display no signs of defective T_{reg} function or activation in vivo, while T_{regs} with disrupted oxidative phosphorylation are impaired in suppressive function and eT_{reg} differentiation. Together, our results highlight the importance of activation-induced Myc function and metabolic reprogramming for orchestrating T_{reg}-suppressive activity in the establishment of immune homeostasis and tolerance.

[1]Department of Immunology, St. Jude Children's Research Hospital, Memphis, TN 38105, USA. [2]Integrated Biomedical Sciences Program, University of Tennessee Health Science Center, Memphis, TN 38163, USA. [3]Department of Pathology, St. Jude Children's Research Hospital, Memphis, TN 38105, USA. [4]Hartwell Center for Bioinformatics and Biotechnology, St. Jude Children's Research Hospital, Memphis, TN 38105, USA. [5]Laboratory of Angiogenesis and Vascular Metabolism, Vesalius Research Center, Department of Oncology, University of Leuven, Leuven, Belgium.
*Present address: Division of Rheumatology, Department of Medicine, and Department of Immunology, Mayo Clinic, Rochester, MN 55905, USA.
†Corresponding author. Email: hongbo.chi@stjude.org

RESULTS

Myc is functionally enriched in neonatal T_{regs} and supports T_{reg} accumulation

Shortly after birth, T cell pools expand and migrate to fill appropriate niches within the lymphopenic host to establish immune homeostasis and tolerance (*21*). T_{regs} play a vital role in this process, and T_{regs} formed during this neonatal period have distinguishable gene expression and effector function compared with those generated during full immune maturity (*22*). To determine important functional mediators of neonatal T_{regs}, we performed gene set enrichment analysis (GSEA) on a deposited dataset of gene profiling of neonatal and adult T_{regs} (*22*). Myc targets were among the most highly enriched gene sets in neonatal T_{regs} (Fig. 1A and fig. S1A), suggesting the preferential up-regulation of Myc function during this important developmental period. Myc expression in neonatal T_{regs} was associated with increased expression of T_{reg}-associated effector molecules, such as ICOS, CTLA4, neuropilin-1 (Nrp-1), CD98, and the proliferative marker Ki-67 (fig. S1B). To further determine Myc expression in T_{regs} during early life, we crossed Myc–GFP (green fluorescent protein) reporter mice (*23*) to Foxp3–RFP (red fluorescent protein) reporter mice (*24*) and compared T_{regs} in different tissues of neonatal (5 to 10 days old) and adult (6 to 8 weeks old) mice. While neonatal mice exhibited decreased T_{reg} frequency in most tissues (except for the liver), Myc-GFP expression was notably increased in neonatal T_{regs} regardless of tissue residence (Fig. 1B and fig. S1C).

To characterize the in vivo role of Myc in T_{regs}, we generated mice with T_{reg}-specific deletion of *Myc* by crossing mice bearing a *Foxp3*-driven Cre recombinase (*25*) with mice containing floxed *Myc* alleles (*Foxp3*^{Cre}*Myc*$^{fl/fl}$) (*26*). Deletion of *Myc* in T_{regs} from *Foxp3*^{Cre}*Myc*$^{fl/fl}$ mice was confirmed by real-time polymerase chain reaction, and Myc-deficient T_{regs} did not display compensatory induction of other Myc family (*Mycn* or *Mycl*) genes (fig. S1D). Myc-deficient T_{regs} displayed a profound reduction in frequency and total numbers (Fig. 1C); this defect was apparent at 7 days of age and continued to increase throughout the early life of the mice (Fig. 1D). Further characterization of T_{regs} in *Foxp3*^{Cre}*Myc*$^{fl/fl}$ mice demonstrated reduced expression of effector molecules in both adult (Fig. 1E) and neonatal animals (fig. S1E). To determine whether these effects were cell intrinsic, we generated mixed bone marrow (BM) chimeras with age-matched wild-type (WT) or *Foxp3*^{Cre}*Myc*$^{fl/fl}$ BM cells and congenic CD45.1$^+$ BM cells at a 1:1 ratio. As compared with WT BM–derived T_{regs}, those from Myc-deficient BM cells showed a drastic reduction in T_{regs} (Fig. 1F and fig. S1F) and defective expression of activation markers (Fig. 1G). Together, these results indicate a cell-intrinsic role of Myc in T_{reg} accumulation and homeostasis.

The cellular mechanisms for loss of T_{regs} may be due to compromised cell survival, proliferation, or lineage stability. The reduction in T_{regs} in *Foxp3*^{Cre}*Myc*$^{fl/fl}$ mice was not attributed to increased cell death, as evidenced by comparable expression of active caspase-3 and annexin V between WT and Myc-deficient T_{regs} (fig. S1G). In contrast, Myc-deficient T_{regs} had severely defective expression of Ki-67 in *Foxp3*^{Cre}*Myc*$^{fl/fl}$ mice and mixed BM chimeras (Fig. 1, H and I). Metabolic dysregulation in T_{regs} can lead to decreased Foxp3 stability and loss of T_{reg} identity (*27*–*29*). To determine whether Myc deficiency was linked to Foxp3 stability, we crossed *Foxp3*^{Cre}*Myc*$^{fl/fl}$ mice to mice bearing *Rosa26*-driven, STOP-"floxed" cassette followed by GFP (*Foxp3*^{Cre}*Myc*$^{fl/fl}$*R26*^{GFP}). This system allows for T_{reg} lineage tracing and determination of "ex-T_{regs}" characterized by *Foxp3*^{Cre}-recombinase–driven GFP expression and loss of Foxp3-YFP expression (i.e., GFP$^+$Foxp3-YFP$^-$). No presence of ex-T_{regs} was observed in *Foxp3*^{Cre}*Myc*$^{fl/fl}$*R26*^{GFP} mice, indicating undisturbed stability (fig. S1H). Thus, Myc function is essential for T_{regs} during neonatal development, and Myc deficiency reduces T_{reg} accumulation likely through defective expansion.

T_{regs} require Myc to control immune homeostasis

T_{regs} generated during neonatal life are critical for immune tolerance (*22*). Consistent with a functional defect of Myc-deficient T_{regs} generated in neonatal life, mice with Myc-deficient T_{regs} developed a severe, early-onset autoimmune disease with death starting to occur at approximately 1 month of age (Fig. 2A). Histological examination revealed an extensive lymphoid/myeloid inflammatory presence in peripheral tissues (Fig. 2B). Also, *Foxp3*^{Cre}*Myc*$^{fl/fl}$ mice showed considerable disruption of T cell homeostasis, with substantially expanded effector (CD62L^{lo}CD44^{hi}) CD4$^+$ and CD8$^+$ populations (Fig. 2C). Significant increases in T helper cell 1 (T_H1; CD4$^+$IFN-γ^+), T_H2 (CD4$^+$IL-4$^+$), and T_H17 (CD4$^+$IL-17$^+$) cells, as well as IFN-γ^+ CD8$^+$ T cells, were observed in *Foxp3*^{Cre}*Myc*$^{fl/fl}$ mice (Fig. 2D). This nonspecific increase in all T_H subsets is in contrast to previous reports using T_{reg}-specific deletion of certain metabolic signaling molecules, with such studies describing a bias in T_H subset inflammation (*13*, *27*, *28*, *30*). Last, the functional suppressive capacity of Myc-deficient T_{regs} was impaired in vitro (fig. S2A). Thus, Myc function is important for ubiquitous T_{reg}-mediated immunosuppressive activity.

Proper T_{reg} effector function is required to restrain germinal center (GC) responses mediated by follicular helper T (T_{FH}) cells (*31*–*33*). *Foxp3*^{Cre}*Myc*$^{fl/fl}$ mice showed increased T_{FH} cells (PD-1^{hi}CXCR5$^+$) and GC B cells (B220$^+$GL-7$^+$Fas$^+$) (Fig. 2, E and F). Moreover, mixed BM chimeric mice displayed a pronounced reduction in Myc-deficient follicular regulatory T (T_{FR}) cells (Fig. 2G), despite the rescue of overall conventional T cell and GC responses due to the presence of CD45.1$^+$-derived cells (fig. S2, B and C). Consistent with the crucial role of Myc in T_{FR} cells, further examination of Myc expression using Myc-GFP reporter mice revealed higher expression levels in CD4$^+$PD-1^{hi}CXCR5$^+$ T cells, with the highest expression observed in T_{FR} cells (Fig. 2H). These results highlight the importance of Myc in T_{reg}-mediated maintenance of GC homeostasis.

T_{reg} maturation and effector programming depend on Myc

To explore the molecular programs controlled by Myc, we purified T_{regs} from WT and *Foxp3*^{Cre}*Myc*$^{fl/fl}$ mice and performed transcriptome analysis. Differential expression analysis showed that there were 331 up-regulated and 159 down-regulated probe sets in Myc-deficient T_{regs} (Fig. 3A). As expected, GSEA revealed that Myc-deficient cells had reductions in Myc target and protein synthesis genes (Fig. 3B). In contrast, enrichment in Myc-deficient T_{regs} mainly included proinflammatory gene sets (Fig. 3B). These results suggest that Myc acts in T_{regs} to enforce T_{reg} function and, ultimately, maintain a proper anti-inflammatory transcriptional signature.

T_{regs} can be classified as eT_{regs} and cT_{regs} (*2*, *34*, *35*) based on their expression of different suppressive and trafficking molecules. eT_{regs} are antigen and activation experienced with enhanced suppressive function and are necessary for overall immune homeostasis (*36*, *37*). We found that Myc-deficient T_{regs} selectively lost signatures associated with eT_{regs} (Fig. 3C) (*37*). Consistent with this observation, detailed analysis of T_{regs} in *Foxp3*^{Cre}*Myc*$^{fl/fl}$ mice revealed a marked decrease in

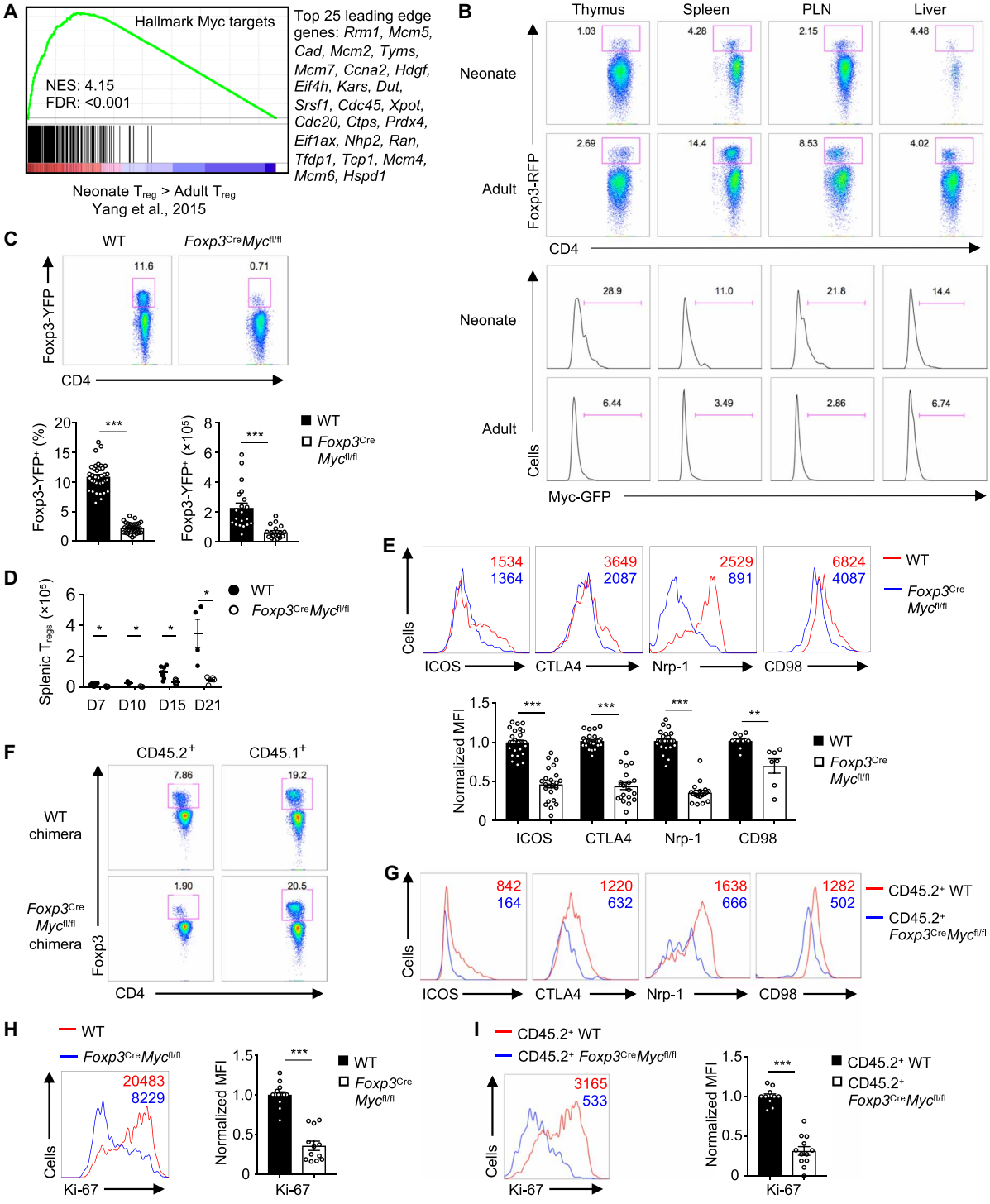

Fig. 1. Myc is functionally enriched in T_{regs} during early immune development, and deficiency of Myc decreases T_{regs} in vivo. (**A**) Gene set enrichment plot of Hallmark Myc targets identified in T_{regs} isolated from neonatal versus adult mice (*22*). (**B**) Flow cytometry analysis of Myc–GFP (green fluorescent protein) expression in $CD4^+Foxp3\text{-}RFP^+$ T_{regs} from indicated tissues in neonatal (5 to 10 days old) and adult (6 to 8 weeks old) $Foxp3^{RFP}$Myc-GFP mice. (**C**) Flow cytometry analysis and quantification of frequency and number of $Foxp3\text{-}YFP^+$ T_{regs} in the spleen of WT and $Foxp3^{Cre}Myc^{fl/fl}$ mice. (**D**) Total splenic T_{reg} numbers on days 7 to 21 after birth in WT and $Foxp3^{Cre}Myc^{fl/fl}$ mice. (**E**) Flow cytometry analysis and quantification [shown as normalized mean fluorescence intensity (MFI) with the expression in WT set as 1] of indicated marker expression in T_{regs} in the spleen of WT and $Foxp3^{Cre}Myc^{fl/fl}$ mice. (**F**) Flow cytometry analysis of Myc-deficient or WT ($CD45.2^+$) and congenic ($CD45.1^+$) $Foxp3^+$ T_{regs} in mixed bone marrow (BM) chimeric mice. (**G**) Flow cytometry analysis of indicated marker expression in splenic $CD45.2^+$ T_{regs} from mixed BM chimeric mice. (**H** and **I**) Flow cytometry analysis and quantification of proliferation marker Ki-67 expression in T_{regs} in the spleen from WT and $Foxp3^{Cre}Myc^{fl/fl}$ (H) or mixed BM chimeric (I) mice. $^*P \leq 0.05$; $^{**}P \leq 0.01$; $^{***}P \leq 0.001$; unpaired Student's *t* test. Data are representative of or pooled from 3 (B), 15 (C, E, and H), 4 (D), or 9 (F, G, and I) independent experiments, with one to four mice per group per experiment. Graphs show means ± SEM. FDR, false discovery rate; NES, normalized enrichment score; PLN, peripheral lymph nodes.

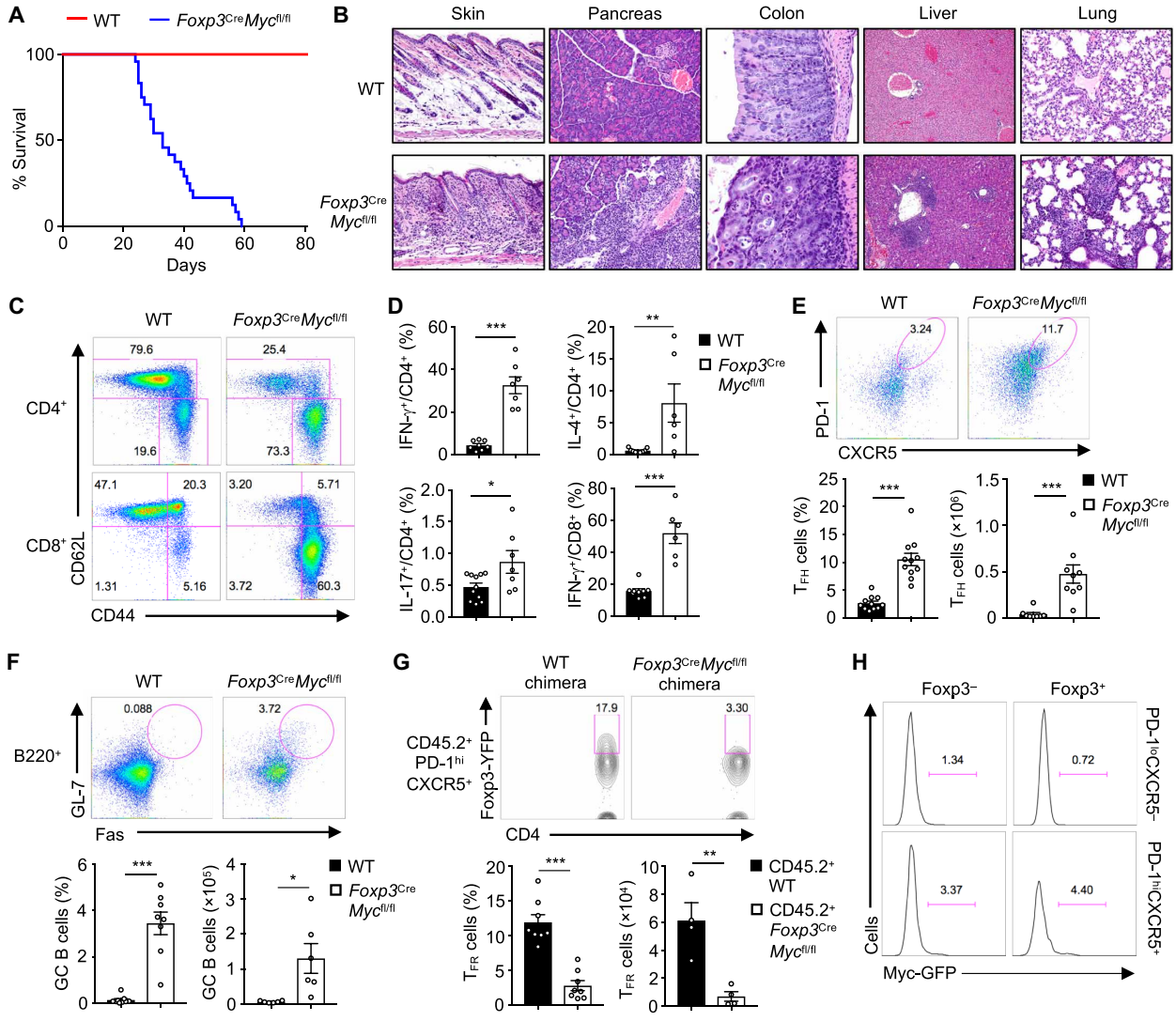

Fig. 2. Deletion of Myc in T_{regs} results in a fatal autoimmune disease and extensively elevated T cell and GC responses. (**A**) Survival curves of *Foxp3*^{Cre}*Myc*$^{fl/fl}$ ($n = 24$) and WT (*Foxp3*^{Cre}*Myc*$^{fl/+}$ and *Foxp3*^{Cre}*Myc*$^{+/+}$) mice ($n = 8$). (**B**) Representative histopathological images from hematoxylin and eosin–stained sections of the indicated tissues (magnification, ×10). (**C**) Flow cytometry analysis of naïve and effector populations of non-T_{reg} CD4$^+$ (denoted as CD4$^+$) and CD8$^+$ T cells in the spleen of WT and *Foxp3*^{Cre}*Myc*$^{fl/fl}$ mice. (**D**) Quantification of cytokine production in splenic T cells of WT and *Foxp3*^{Cre}*Myc*$^{fl/fl}$ mice. (**E** to **G**) Flow cytometry analysis and quantification of frequencies and total numbers of CD4$^+$PD-1^{hi}CXCR5$^+$ follicular helper T (T_{FH}) cells (E) and B220$^+$GL-7$^+$Fas$^+$ GC B cells (F) in the spleen of WT and *Foxp3*^{Cre}*Myc*$^{fl/fl}$ mice, or follicular regulatory T (T_{FR}) cells in mixed BM chimeric mice (G). (**H**) Flow cytometry analysis of Myc-GFP expression within indicated CD4$^+$ subsets in *Foxp3*^{RFP}Myc-GFP mice. *$P \leq 0.05$; **$P \leq 0.01$; ***$P \leq 0.001$; unpaired Student's *t* test. Data are representative of or pooled from 15 (C), 5 (D and G), 7 (E and F), or 2 (H) independent experiments, with one to four mice per genotype per experiment. Graphs show means ± SEM.

eT_{regs} (CD62L^{lo}CD44^{hi}) (Fig. 3D). A similar observation was made for the expression of the T_{reg} activation–associated marker KLRG1 (Fig. 3E). The reduction in Myc-deficient eT_{regs} was prevalent in mixed BM chimeras (Fig. 3F), supportive of a cell-intrinsic mechanism.

Myc is involved in a vast array of important cellular processes, and its expression is tightly regulated. We observed that Myc expression was temporally regulated during development (Fig. 1B). To determine whether improper Myc regulation could affect T_{reg} accumulation or function, we used mice harboring a *Myc* transgene preceded by a STOP-floxed cassette on the *Rosa26* locus (*38*). When crossed with *Foxp3*^{Cre} mice, this results in constitutive Myc transgene expression specifically in T_{regs} (*Foxp3*^{Cre}*R26*^{MYC}). Unexpectedly, *Foxp3*^{Cre}*R26*^{MYC} mice showed no noticeable differences in frequencies of total T_{regs} (fig. S3A) or eT_{regs} (fig. S3B) at steady state. T_{reg} effector molecule expression was largely unaltered, except for Ki-67, which was markedly elevated in T_{regs} from *Foxp3*^{Cre}*R26*^{MYC} mice (fig. S3C). Myc overexpression in T_{regs} had no effect on CD4$^+$ or CD8$^+$ T cell homeostasis (fig. S3D) or GC responses (fig. S3E), consistent with normal suppressive capacity in vitro (fig. S3F). These data suggest a more nuanced, context-dependent role of Myc in T_{reg} function and homeostasis; while deficiency of Myc impairs T_{reg} function and eT_{reg} accumulation in vivo, Myc overexpression alone is not sufficient to alter immune homeostasis.

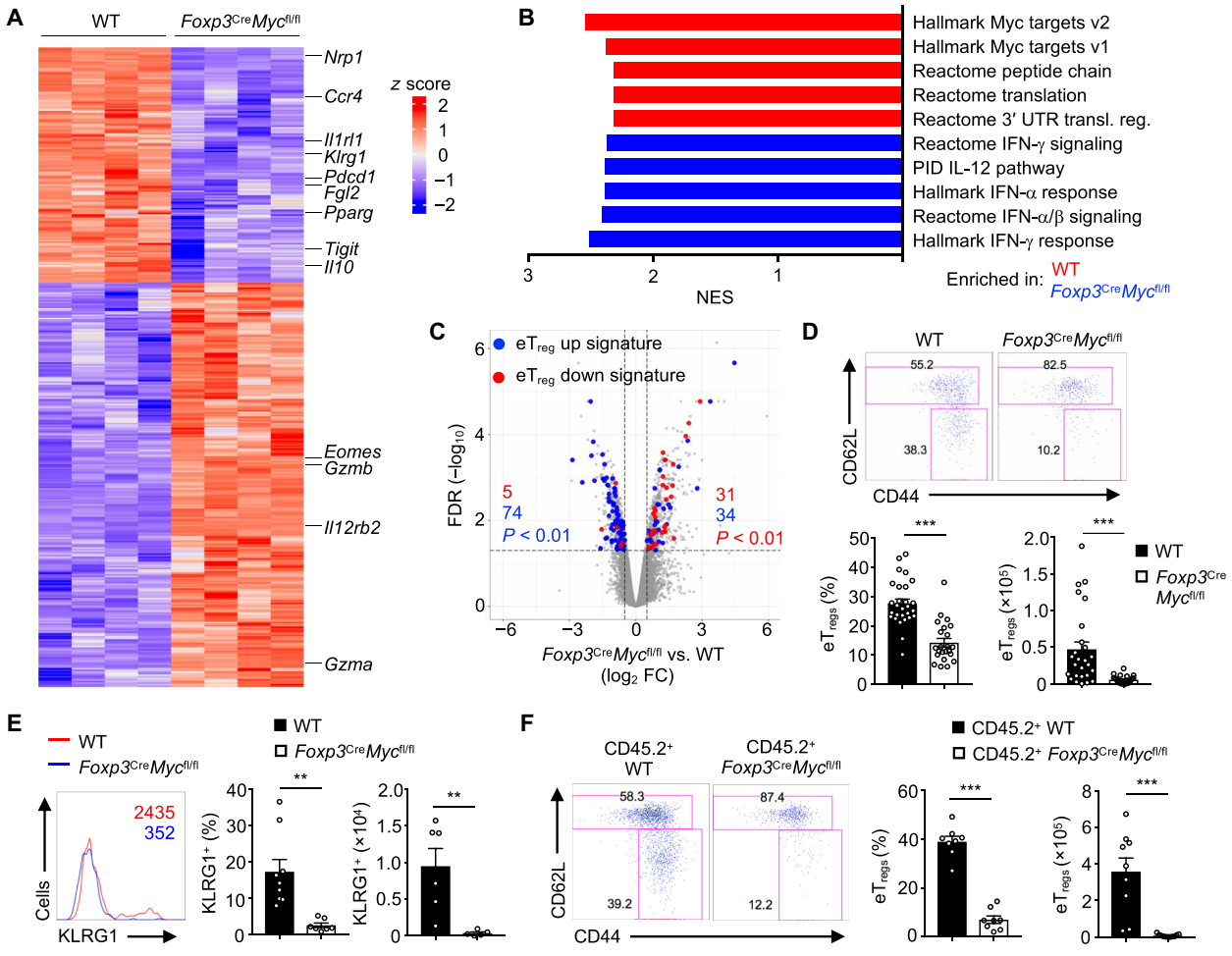

Fig. 3. Loss of Myc dampens eT$_{reg}$ gene signature and generation. (**A**) Heatmap of differentially expressed (DE; fold change, >2) genes in T$_{regs}$ from WT and *Foxp3*^{Cre}*Myc*$^{fl/fl}$ mixed BM chimeric mice. (**B**) Top five gene sets differentially enriched by normalized enrichment score (NES) in WT (red) or Myc-deficient (blue) T$_{regs}$. (**C**) Volcano plot of DE genes from WT and Myc-deficient T$_{regs}$ with number of genes correlating with eT$_{reg}$ gene signature (genes up-regulated in eT$_{regs}$, blue; genes down-regulated in eT$_{regs}$, red) (*37*). (**D**) Flow cytometry analysis of cT$_{regs}$ (CD62L^{hi}CD44^{lo}) and eT$_{regs}$ (CD62L^{lo}CD44^{hi}) (gated on CD4$^+$Foxp3-YFP$^+$) and quantification of frequency and number of splenic T$_{regs}$ in WT and *Foxp3*^{Cre}*Myc*$^{fl/fl}$ mice. (**E**) Flow cytometry analysis and quantification of KLRG1 expression on total T$_{regs}$ in the spleen of WT and *Foxp3*^{Cre}*Myc*$^{fl/fl}$ mice. (**F**) Flow cytometry analysis of cT$_{regs}$ and eT$_{regs}$ and quantification of frequency and number of splenic eT$_{regs}$ in mixed BM chimeras. $^{**}P \leq 0.01$; $^{***}P \leq 0.001$; χ^2 square test (C) or unpaired Student's *t* test (D to F). Data are representative of or pooled from 15 (D) or 6 (E and F) independent experiments, with one to three mice per group per experiment. Graphs show means ± SEM.

Myc-deficient T$_{regs}$ fail to expand and control acute inflammation

Inflammation causes T$_{regs}$ to undergo a transient activation program that increases their suppressive activity and expansion (*34*, *39*). Our previous work identified the important role of Myc in the activation of conventional CD4$^+$ and CD8$^+$ T cells (*9*). To investigate a role in T$_{regs}$, we performed GSEA on two published datasets containing acutely activated T$_{regs}$ and resting T$_{regs}$ (*34*, *39*). Expression of Myc target genes was highly enriched in activated T$_{regs}$ from both datasets (Fig. 4A), suggesting a role of Myc in supporting the activation/effector program of T$_{regs}$. This functional importance of Myc likely extends to various pathological conditions, as we observed an increase of Myc expression and Myc$^+$ T$_{regs}$ in the spinal cords of mice with experimental autoimmune encephalomyelitis (EAE) (fig. S4A) and also among tumor-infiltrating lymphocytes of mice inoculated with MC38 adenocarcinoma cells (fig. S4B).

To directly test how Myc-deficient T$_{regs}$ respond to inflammatory stimuli, we used a well-characterized in vivo model of acute inflammation via transient T$_{reg}$ depletion (*34*, *40*). In this system, mosaic female mice (see Materials and Methods) have ~50% T$_{regs}$ that express the receptor for diphtheria toxin (DT) and ~50% T$_{regs}$ that are Myc deficient (or WT T$_{regs}$ as control). These mice do not have aberrant inflammation at steady state (fig. S4C). Upon DT injection, the DT receptor (DTR)–expressing T$_{regs}$ are depleted, leaving the remaining T$_{regs}$ to respond to the resulting inflammation (Fig. 4B). Upon DT injection, Myc-deficient T$_{regs}$ (YFP$^+$) failed to expand to the same extent as WT T$_{regs}$ (Fig. 4C). Furthermore, eT$_{reg}$ accumulation was enhanced in WT T$_{regs}$ but was markedly impaired in those lacking Myc (Fig. 4D). This impairment was concomitant with increases in effector CD4$^+$ and CD8$^+$ populations (Fig. 4E) and T$_H$1, T$_H$2, and T$_H$17 responses (Fig. 4F). Expression of T$_{reg}$ effector molecules was variable in this model (fig. S4D),

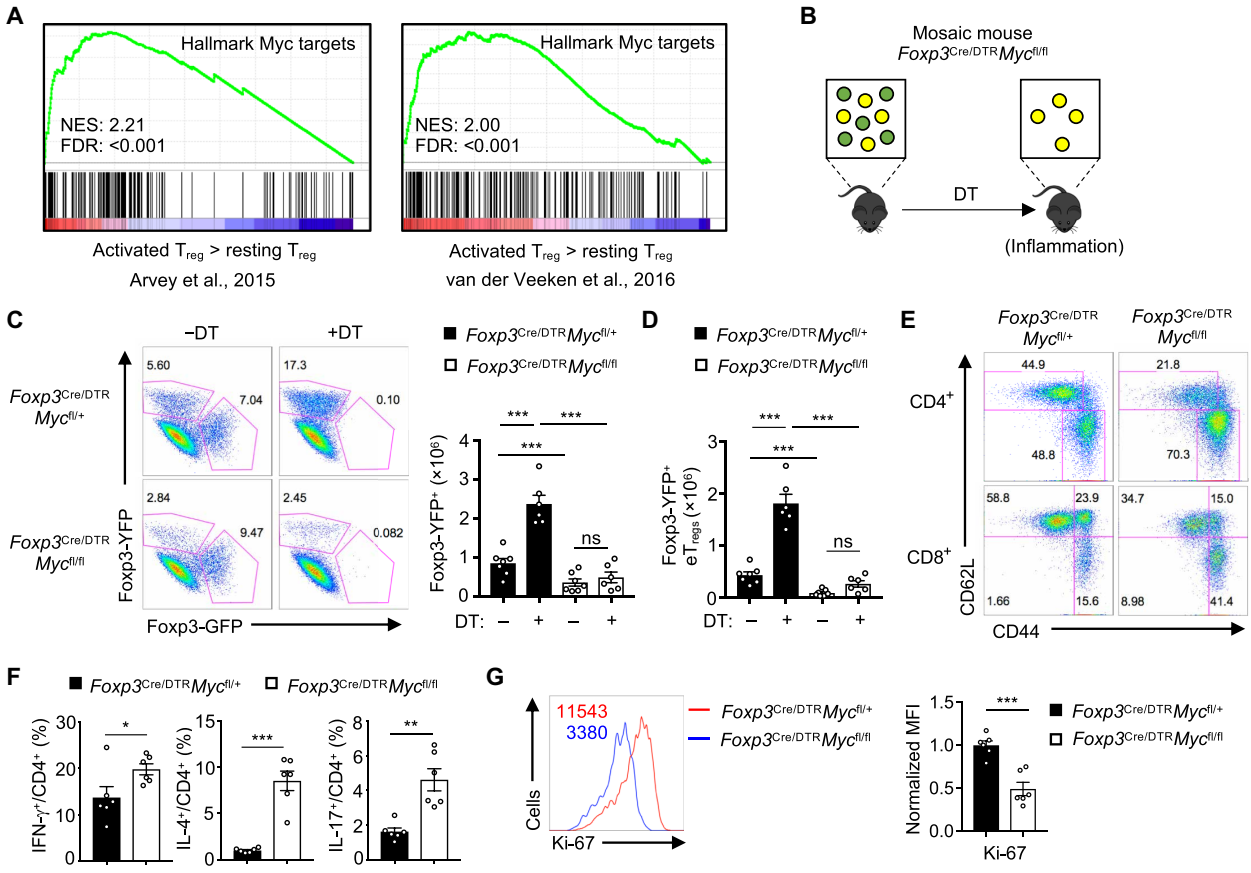

Fig. 4. Myc-deficient T_{regs} fail to expand and control acute inflammation. (**A**) Enrichment of Hallmark Myc target gene set in activated and resting T_{regs} from published datasets (*34*, *39*). (**B**) Schematic of diphtheria toxin (DT)–mediated T_{reg} depletion in Foxp3-DTR (DT receptor) mosaic mice. (**C**) Flow cytometry analysis and quantification of WT/Myc-deficient (YFP^+) and DTR^+ (GFP^+) T_{regs} before and after DT treatment in mosaic mice. (**D**) Quantification of eT_{reg} number. (**E**) Flow cytometry analysis of naïve and effector populations of non-T_{reg} $CD4^+$ and $CD8^+$ T cells. (**F**) Quantification of cytokine production in T_H subsets in the spleen. (**G**) Flow cytometry analysis and quantification of Ki-67 expression in $CD4^+Foxp3\text{-}YFP^+$ T_{regs} in DT-treated mosaic mice. $^*P \le 0.05$; $^{**}P \le 0.01$; $^{***}P \le 0.001$; ns, not significant; unpaired Student's *t* test. Data are representative of or pooled from two independent experiments, with three to four mice per group per experiment. Graphs show means ± SEM. FDR, false discovery rate; NES, normalized enrichment score.

but Ki-67 showed consistently decreased expression in Myc-deficient T_{regs} (Fig. 4G). These results establish that Myc deficiency is detrimental for eT_{reg} generation and suppressive function during acute inflammation.

Myc is required for transition to, but not maintenance of, eT_{regs}

T_{regs} require continuous T cell receptor (TCR) signals to establish and maintain the eT_{reg} program and immune tolerance (*36*, *37*). Because Myc expression and transcriptional programs are induced by TCR-dependent signals (*9*, *41*), we next determined the temporal requirements for Myc expression in eT_{reg} accumulation. To this end, we crossed $Myc^{fl/fl}$ mice with a tamoxifen-inducible Foxp3-Cre recombinase [$Foxp3^{Cre\text{-}ERT2}Myc^{fl/fl}$ (*42*)]. In this system, T_{regs} maintain "normal" Myc functional capacity until mice are injected with tamoxifen, which allows Cre-mediated gene deletion to occur. In contrast to the severe inflammatory phenotype of $Foxp3^{Cre}Myc^{fl/fl}$ or DT-treated $Foxp3^{Cre/DTR}Myc^{fl/fl}$ mice, $Foxp3^{Cre\text{-}ERT2}Myc^{fl/fl}$ mice showed no signs of aberrant inflammation following tamoxifen-induced *Myc* deletion in T_{regs} (fig. S4, E and F), which was not attributed to elevated expression of *Mycn* or *Mycl* (fig. S4E). Notably, induced deletion of *Myc* had no effect on eT_{reg} percentage, although $KLRG1^+$ T_{regs} trended slightly lower (Fig. 5A). These results were unexpected, given the drastic eT_{reg} phenotype observed in the constitutive deletion model, $Foxp3^{Cre}Myc^{fl/fl}$ mice.

We hypothesized that Myc function may be more important for T_{reg} activation (i.e., during transition from cT_{regs} to eT_{regs}) rather than for the maintenance of eT_{regs}. To test this, we used a previously published model of in vitro T_{reg} activation (*13*, *43*). We again used tamoxifen-injected $Foxp3^{Cre\text{-}ERT2}Myc^{fl/fl}$ mice to sort GFP^+ $YFP^+CD62L^{hi}CD44^{lo}$ cT_{regs}, followed by 3 days of stimulation with anti-CD3/CD28 antibodies and interleukin-2 (IL-2) (Fig. 5B). Examination of activation-associated parameters CD44 (marker associated with eT_{reg} generation in vitro) and cell size (forward scatter area; FSC-A) revealed an inability of Myc-deficient T_{regs} to increase both of these markers following stimulation (Fig. 5B). Furthermore, pharmacological inhibition of Myc with either JQ-1 or i-BET-762 (*29*) in stimulated cT_{regs} from WT mice caused a similar blunting effect on T_{reg} activation (Fig. 5C). Last, cT_{regs} from $Foxp3^{Cre}R26^{MYC}$ mice (with constitutive Myc expression) showed a consistent increase in CD44 and cell size following in vitro stimulation (Fig. 5D). These results show that T_{reg} use of Myc occurs primarily during activation, while Myc function is dispensable for eT_{reg} maintenance.

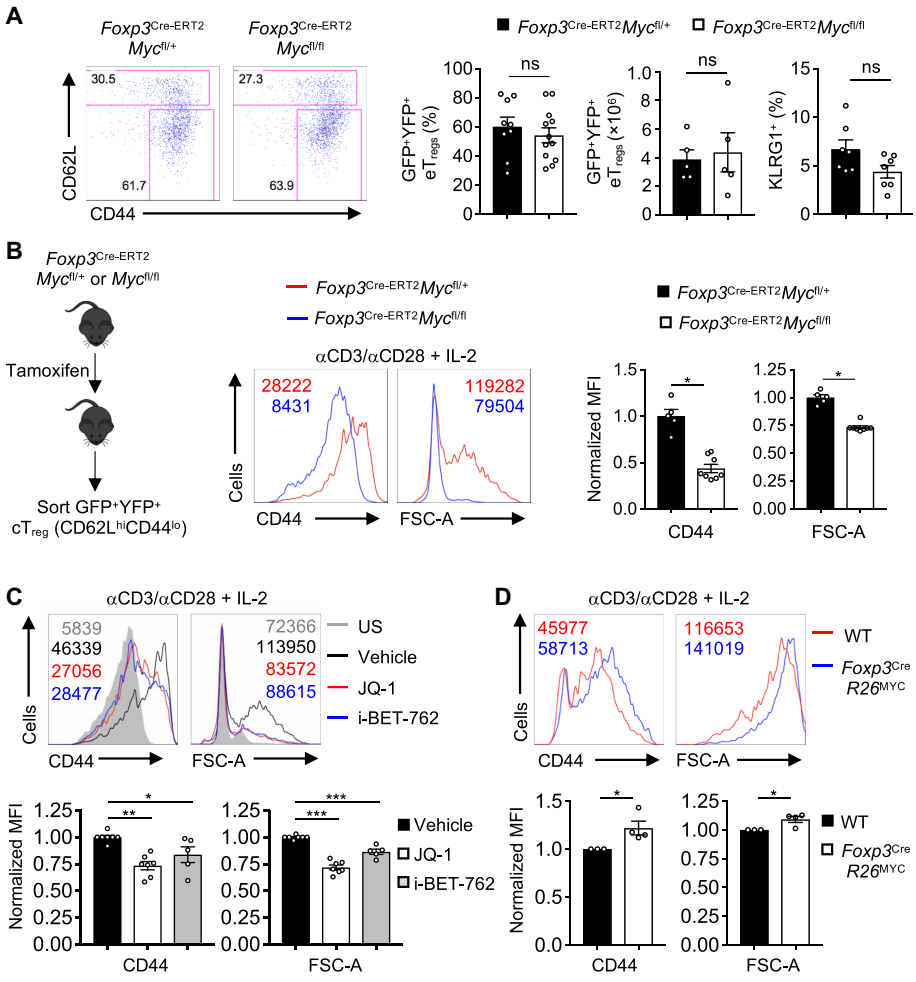

Fig. 5. Acute deletion of Myc reveals the requirement of Myc for transition to, but not maintenance of, eT$_{regs}$. (**A**) Flow cytometry analysis of cT$_{regs}$ and eT$_{regs}$, and quantification of frequency and number of eT$_{regs}$ and KLRG1 expression on T$_{regs}$ in the spleen of *Foxp3*$^{Cre\text{-}ERT2}$*Myc*$^{fl/+}$ and *Foxp3*$^{Cre\text{-}ERT2}$*Myc*$^{fl/fl}$ mice treated with tamoxifen (2 mg per injection every other day for a total of six injections; analysis was performed 21 days after the final injection). Plots are pregated on Foxp3-GFP$^+$ T$_{regs}$ also reporting YFP$^+$ for successful Cre-mediated recombination (CD4$^+$GFP$^+$YFP$^+$). (**B**) Schematic with representative and quantified results for in vitro activation of cT$_{regs}$ (CD4$^+$GFP$^+$YFP$^+$CD62L^{hi}CD44^{lo}) sorted from 8-week-old *Foxp3*$^{Cre\text{-}ERT2}$*Myc*$^{fl/+}$ and *Foxp3*$^{Cre\text{-}ERT2}$*Myc*$^{fl/fl}$ mice treated with tamoxifen as in (A). (**C**) Effects of Myc inhibitors JQ-1 (500 nM) and i-BET-762 (500 nM) on in vitro activation of WT cT$_{regs}$ (CD4$^+$YFP$^+$CD62L^{hi}CD44^{lo}) sort purified from 6- to 8-week-old mice. (**D**) In vitro activation of Myc-overexpressing cT$_{regs}$ from 6- to 8-week-old WT and *Foxp3*^{Cre}*R26*^{MYC} mice. *$P \leq 0.05$; **$P \leq 0.01$; ***$P \leq 0.001$; ns, not significant; unpaired Student's *t* test. Data are representative of or pooled from four (A, C, and D) or two (B) independent experiments, with one to three mice per group per experiment. Graphs show means ± SEM. Forward scatter area, FSC-A.

FAO-independent oxidative metabolism contributes to T$_{reg}$ function and eT$_{reg}$ generation

Our data demonstrating the importance of Myc function in proper activation of T$_{regs}$ led us to consider current paradigms of metabolic regulation in T$_{regs}$. We have recently shown an essential role of mitochondrial function for T$_{reg}$ suppressive activity (*13*), and GSEA of Myc-deficient T$_{regs}$ showed a reduction for the Hallmark oxidative phosphorylation pathway (Fig. 6A). To investigate the direct activity of Myc in mitochondrial function, we overlaid Myc target genes [generated from a published chromatin immunoprecipitation sequencing (ChIP-seq) dataset in T cells (*10*)] and mitochondria-related genes [identified by the MitoCarta 2.0 database (*44*)], with differentially expressed genes between WT and Myc-deficient T$_{regs}$ (fig. S5A). Direct Myc targets based on the ChIP-seq dataset represented 111 of 526 genes (~21%) that were down-regulated in Myc-deficient T$_{regs}$. Further, direct Myc targets represented 219 of 1158 (~19%) of the MitoCarta 2.0 gene set, with 19 of 53 of the mitochondrial genes that were down-regulated in Myc-deficient T$_{regs}$ representing direct Myc targets. In contrast, there was little overlap between the direct Myc targets, MitoCarta 2.0 genes, and genes up-regulated in Myc-deficient T$_{regs}$. These data indicate that Myc can directly promote mitochondrial metabolism to support T$_{reg}$ function. Consistent with this notion, Myc function was important for mitochondrial function, as indicated by the reduced oxygen consumption rate (OCR) in T$_{regs}$ activated in vitro in the presence of Myc inhibitors (Fig. 6B). In addition, extracellular acidification rate (ECAR) was decreased (fig. S5B). Direct perturbation of mitochondrial oxidative phosphorylation by deleting *Cox10* (fig. S5, C and D) (*45*) further revealed the importance of this metabolic pathway in T$_{reg}$ function and eT$_{reg}$ generation. Specifically, *Foxp3*^{Cre}*Cox10*$^{fl/fl}$ mice showed reduced proportions of T$_{regs}$ (Fig. 6C) and increased activation (Fig. 6D) and cytokine production (fig. S5E) by CD4$^+$ and

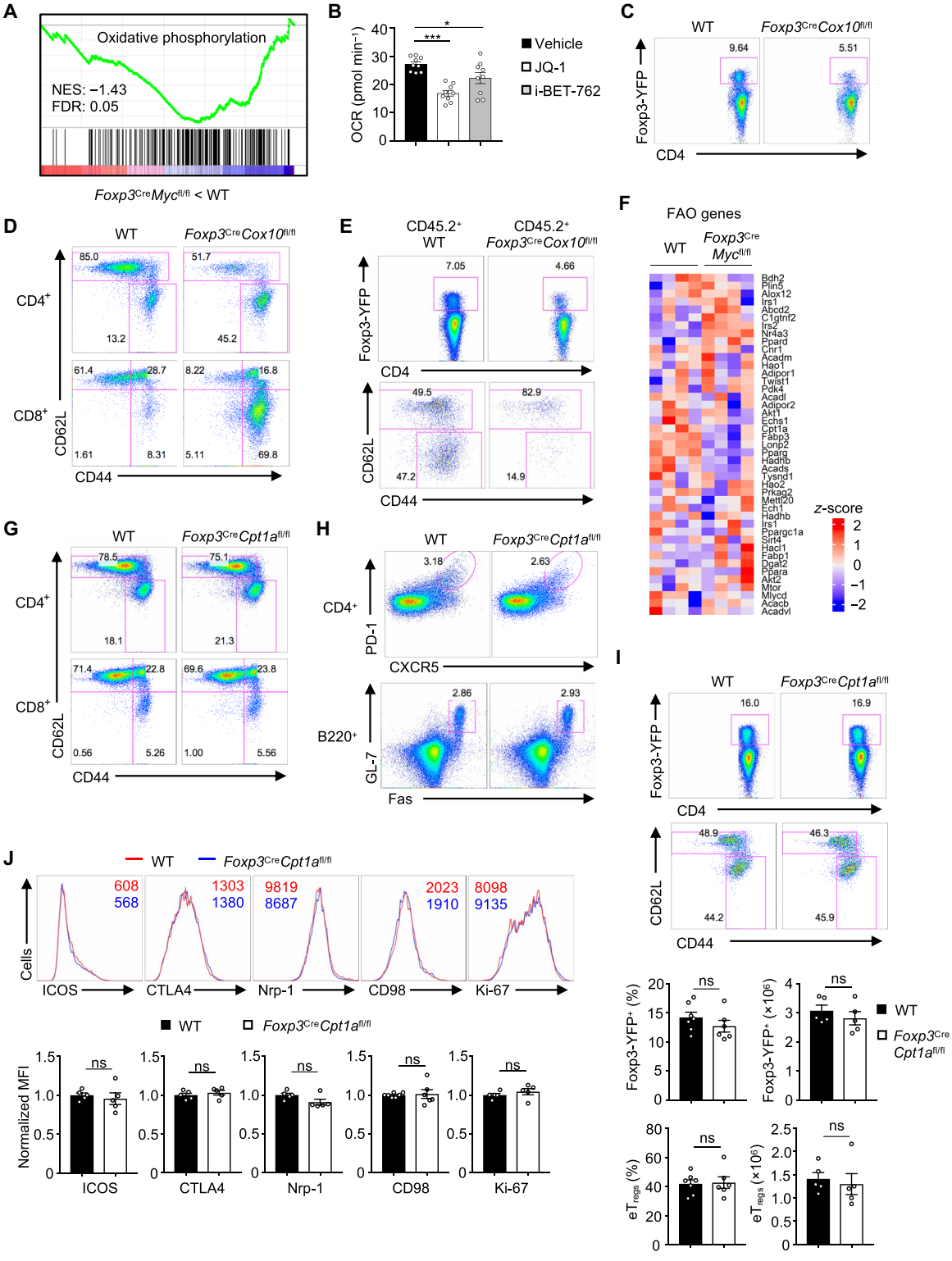

Fig. 6. Oxidative metabolism contributes to T_{reg} function and eT_{reg} generation, while FAO is dispensable. (**A**) Negative enrichment of Hallmark oxidative phosphorylation gene set in Myc-deficient T_{regs}. (**B**) Oxygen consumption rate (OCR) in T_{regs} activated in the presence of Myc inhibitors JQ-1 (1 μM) or i-BET-762 (1 μM). (**C** and **D**) Flow cytometry analysis of splenic T_{regs} (C) and naïve and effector $CD4^+$ and $CD8^+$ T cells (D) in WT and *Foxp3*^{Cre}*Cox10*$^{fl/fl}$ mice. (**E**) Flow cytometry analysis of total splenic T_{regs} and cT_{regs} and eT_{regs} in mixed BM chimeras. (**F**) Heatmap of expression of FAO-related genes. (**G** to **J**) Flow cytometry analysis of naïve and effector $CD4^+$ and $CD8^+$ T cells (G), GC responses (H), total T_{regs}, cT_{regs}, and eT_{regs} (I), and marker and Ki-67 expression in T_{regs} (J) in the spleen of WT and *Foxp3*^{Cre}*Cpt1a*$^{fl/fl}$ mice. $^*P \leq 0.05$; $^{***}P \leq 0.001$; ns, not significant; unpaired Student's *t*-test. Data are representative of five independent experiments, with one to two mice per group per experiment. FDR, false discovery rate; NES, normalized enrichment score.

$CD8^+$ T cells. Cox10-deficient T_{regs} showed impaired suppression in vitro (fig. S5F). Reductions in overall proportions of Cox10-deficient T_{regs} and eT_{regs} (Fig. 6E) were observed in mixed BM chimeras, supportive of a cell-intrinsic defect. Thus, Myc is an essential transcriptional regulator of mitochondrial metabolism in T_{regs}, and impaired mitochondrial oxidative phosphorylation in T_{regs} is sufficient to disrupt T_{reg} accumulation and eT_{reg} generation.

On the basis of pharmacological studies, FAO is a preferred metabolic pathway for driving mitochondrial function in T_{regs} (*14*), yet the regulation and in vivo function of this pathway remain poorly understood. We found that Myc-deficient T_{regs} did not have alteration of FAO-related genes (Fig. 6F), suggesting that Myc likely regulates mitochondrial function independently of FAO. To investigate the role of FAO in T_{reg}-mediated immune homeostasis in vivo, we crossed *Foxp3*^{Cre} mice to mice bearing floxed *Cpt1a* alleles (*46*), where we observed a specific reduction in *Cpt1a* but no changes in *Cpt1b* or *Cpt1c* (fig. S5G). T_{regs} from *Foxp3*^{Cre}*Cpt1a*$^{fl/fl}$ mice were confirmed to have functionally defective FAO when using palmitate bovine serum albumin (BSA) as a substrate for oxidative phosphorylation (fig. S5H). Mice with Cpt1a-deficient T_{regs} did not show aberrant $CD4^+$ or $CD8^+$ T cell activation (Fig. 6G), cytokine production (fig. S5I), or GC responses (Fig. 6H and fig. S5J). Also, *Foxp3*^{Cre}*Cpt1a*$^{fl/fl}$ mice had undisturbed cellularity of total T_{regs} and eT_{regs} (Fig. 6I), with normal T_{reg} effector marker and Ki-67 expression (Fig. 6J). Last, Cpt1a deficiency in T_{regs} had no effect on in vitro suppressive capacity (fig. S5K). These data suggest that FAO is a dispensable component of T_{reg} development and function.

DISCUSSION

Myc is one of the most comprehensively studied molecules in cancer biology due to its broad functional scope and ubiquitous expression among diverse cell types (*47*). In physiological contexts, namely, activation of conventional $CD4^+$ and $CD8^+$ T cells, Myc facilitates metabolic reprogramming necessary for exit from quiescence (*9*). However, in T_{regs}, a metabolically unique cell type from conventional T cells (*5*, *7*, *11*, *12*), Myc expression and function have been shown to be actively repressed by Foxp3 to exert immune tolerance (*17*). Therefore, the functional role and regulation of Myc in T_{regs} remain uncertain.

Our data show that the T_{reg} pool in *Foxp3*^{Cre}*Myc*$^{fl/fl}$ mice does not adequately expand during early neonatal development, a critical tuning period of the immune system (*21*). Without an effective counterbalance, proinflammatory inflammation causes tissue damage and leads to early death in *Foxp3*^{Cre}*Myc*$^{fl/fl}$ mice. Whereas *Foxp3*^{Cre}*Myc*$^{fl/fl}$ mice contain $Foxp3^+$ T_{regs} (albeit at much lower numbers), the severity of autoimmune disease, early onset of lethality, and aberrant GC responses are comparable to *Foxp3* null, "Scurfy" mice that harbor no T_{regs} (*32*, *48*). Furthermore, our in vitro T_{reg} suppression data suggest that Myc-deficient T_{regs} are unable to control inflammation. Transcriptome analysis reveals that Myc-deficient T_{regs} have reduced expression of the eT_{reg} gene signature, which is consistent with our flow cytometry findings. We also find that Myc function is important for T_{regs} during acute inflammatory responses. Unlike the comparison of WT and *Foxp3*^{Cre}*Myc*$^{fl/fl}$ mice, the DT-mediated mosaic T_{reg} depletion model illustrates a critical response-reactive mechanism wherein T_{regs} are "forced" to confront a proinflammatory environment within a physiological context. The failure of Myc-deficient T_{regs} to expand or undergo transitional activation to become eT_{regs}, and the consequential inability to subdue effector T cell responses, is consistent with the enrichment of Myc target genes in activated T_{regs}. Together, these results suggest that Myc-dependent T_{reg} activation and eT_{reg} population establishment are crucial components of early immune development and acute inflammation.

We describe several negative findings in this study that were originally surprising. Our data show that Myc is required for cT_{reg} transition into eT_{reg} but is dispensable in maintaining eT_{reg} identity, based on the analysis of the tamoxifen-treated *Foxp3*$^{Cre\text{-}ERT2}$*Myc*$^{fl/fl}$ mouse model. Previous work in conventional T lymphocytes and embryonic stem cells has argued that Myc has no direct impact on specification nor reprogramming of cell differentiation and instead serves as an "amplifier" of predicated transcriptional programs (*10*), although this notion has been recently challenged (*49*, *50*). We propose that upon activation, T_{regs} transiently express Myc to boost expression of genes involved in providing a bolus of nutrients and proteins, which facilitates exit from quiescence. Moreover, we observe no substantial alterations in immune homeostasis or T_{regs} (except for increased Ki-67 expression) in *Foxp3*^{Cre}*R26*^{MYC} mice. However, Myc-overexpressing T_{regs} from these mice show enhanced activation in vitro, suggesting that Myc function in T_{regs} is highly context dependent (i.e., only during activation) and ectopic Myc expression is not sufficient to alter baseline function. In one previous study supporting this notion, enforced expression of Myc was oncogenic within regenerating (metabolically active) livers but not within fully grown (metabolic steady state) adult livers (*51*).

Our previous work described the important role of Myc in the metabolic reprogramming of naïve $CD4^+$ and $CD8^+$ T cells upon activation. In the absence of Myc, these cells are unable to up-regulate anabolic pathways, but quiescence-associated pathways such as FAO are unaffected (*9*). It has been proposed that T_{reg} function is reliant on mitochondrial metabolism driven by FAO, akin to memory and naïve T cells with low metabolic activity (*14*). However, this idea has recently been disputed (*19*, *20*). T_{reg}-specific impairment of oxidative phosphorylation in *Foxp3*^{Cre}*Cox10*$^{fl/fl}$ mice results in an autoimmune disease, consistent with cell-intrinsic decreases in eT_{regs} and in vitro suppressive capacity. In contrast, we show here that mice with T_{reg}-specific Cpt1a deficiency show no signs of abnormal immune regulation nor T_{reg} homeostasis, in line with the model of Cpt1a deficiency in all T lymphocytes (*19*). Literature addressing the role of anabolic metabolism in T_{reg} function has revealed a relationship that is more complex than previously thought (*13*, *18*, *27*, *28*, *52*). Increasing anabolic metabolism through enforced expression of Glut1 or constitutively active Akt (*18*), or deletion of PTEN (phosphatase and tensin homolog) (*27*, *28*), results in T_{reg} hyperproliferation but diminished suppressive function, owing to the impaired lineage stability. In contrast, decreased anabolic metabolism through deletion of Mtor (*13*) or Raptor (*52*) leads to defective proliferation and eT_{reg} generation, which is phenotypically similar to Myc deficiency in T_{regs}. By analyzing Cox10-deficient T_{regs}, we further reveal a crucial requirement of oxidative phosphorylation for T_{reg} function and eT_{reg} generation. Future research is warranted to dissect the specific metabolic programs underpinning oxidative phosphorylation.

In summation, Myc function is central for proper T_{reg} accumulation, activation, and effector function. The results of this current study highlight metabolic reprogramming as a major determinant of T_{reg} functional potency in the contexts of inflammation and during early development.

MATERIALS AND METHODS

Mice

C57BL/6, CD45.1$^+$, *Cox10*$^{fl/fl}$, *Rag1*$^{-/-}$, *Foxp3*^{RFP}, *Foxp3*$^{DTR\text{-}GFP}$, *R26*^{MYC}, *R26*^{YFP} reporter, and *R26*^{GFP} reporter (a *loxP* site–flanked STOP cassette followed by the YFP- or GFP-encoding sequence inserted into the *Rosa26* locus) mice were purchased from the Jackson laboratory. *Foxp3*$^{YFP\text{-}Cre}$ (*25*) and *Foxp3*$^{Cre\text{-}ERT2}$ (*42*) mice were gifts from A. Rudensky. *Myc*$^{fl/fl}$ mice (*9*) were gifts from D.R. Green and F.W. Alt. Myc-GFP reporter mice (*23*) were gifts from B. Sleckman. *Foxp3*^{Cre}*Myc*$^{fl/fl}$ mice were used at 2 to 3 weeks old, with age- and gender-matched control mice. Other mice were used at 8 to 10 weeks old, unless otherwise noted. Mixed BM chimeric mice were generated by adoptively transferring a 1:1 mix of CD45.1$^+$ spike and CD45.2$^+$ (*Foxp3*^{Cre}*Myc*$^{fl/+}$ or *Foxp3*^{Cre}*Myc*$^{fl/fl}$) T cell–depleted BM cells into sublethally irradiated (5.5 Gy) *Rag1*$^{-/-}$ mice, followed by at least 8 weeks of reconstitution. For T_{reg} depletion experiments, *Myc*$^{fl/+}$ and *Myc*$^{fl/fl}$ female mosaic mice (harboring a *Foxp3*$^{DTR\text{-}GFP}$ allele on one X chromosome and *Foxp3*^{Cre} allele on the other X chromosome) were injected intraperitoneally with DT (50 μg kg^{-1}; EMD Millipore) every other day for four total injections and then analyzed 3 days after the last injection. For tamoxifen administration, mice were injected intraperitoneally with tamoxifen (2 mg per mouse) in corn oil every other day for six total injections and then analyzed 3 weeks after the last injection. All mice were kept in a specific pathogen–free facility in the Animal Resource Center at St. Jude Children's Research Hospital, and animal protocols were approved by the Institutional Animal Care and Use Committee.

Flow cytometry

For analysis of surface markers, cells were stained in phosphate-buffered saline containing 2% (w/v) BSA. The following fluorescent-labeled antibodies (purchased from Thermo Fisher Scientific, Tonbo, BD Biosciences, Cell Signaling Technology, and Sony Biotechnology) were used: anti-CD4 (RM4-5), anti-CD8 (53-6.7), anti-CD25 (PC61.5), anti-B220 (RA3-6B2), anti-CD62L (MEL-14), anti-CD44 (IM7), anti-Fas (Jo2), anti-GL7 (GL-7), anti–PD-1 (J43), anti-ICOS (C398.4A), anti–Nrp-1 (3DS304M), anti-CD98 (RL388), anti-CD45.1 (A20), anti-CD45.2 (104), anti-KLRG1 (2F1), and anti-TCRβ (H57–597). Biotin-conjugated anti-CXCR5 (2G8) antibody and phycoerythrin (PE)–labeled streptavidin from BD Biosciences were used for T_{FH} staining. Active caspase-3 or annexin V staining was performed according to the manufacturer's instructions (BD Biosciences). For intracellular staining, cells were fixed using the Foxp3 fixation buffer (Thermo Fisher Scientific) as per the manufacturer's instructions. The following antibodies were used: anti-Foxp3 (FJK-16 s), anti-CTLA4 (UC10-4B9), anti–Ki-67 (SolA15), anti–c-Myc (D84C12), anti–interferon-γ (IFN-γ) (XMG1.2), anti–IL-17A (TC11-18H10.1), and anti–IL-4 (11B11). For intracellular cytokine staining, cells were stimulated for 4 to 5 hours with phorbol 12-myristate 13-acetate and ionomycin in the presence of monensin (BD Biosciences). Flow cytometry data were collected using LSRII or Fortessa (BD Biosciences) cytometers and analyzed with FlowJo v10 software (TreeStar). Fluorescence-activated cell sorting was performed using Synergy or Reflection instruments (Sony Biotechnology).

Histology

Tissue samples were fixed in 10% neutral-buffered formalin, paraffin embedded, sectioned, and then stained with hematoxylin and eosin. All analyses were performed by an experienced pathologist (P.V.) in a blinded manner.

Cell culture

For cT_{reg} activation, sort-purified cells were cultured for 3 days in complete Click's medium [10% fetal bovine serum (FBS), 1% penicillin/streptomycin + L-glutamine, β-mercaptoethanol] with anti-CD3 (5 μg ml^{-1}; plate bound), anti-CD28 (5 μg ml^{-1}), and IL-2 (100 U ml^{-1}). In some experiments, pharmacological Myc inhibitor JQ-1 (500 nM) or i-BET-762 (500 nM) was added to the culture. For in vitro T_{reg} suppression assays, purified T_{regs} were cocultured with naïve CD4$^+$ T cells and irradiated splenocytes as previously described (*13*).

EAE model

Mice were subcutaneously immunized with 200 μg of myelin oligodendrocyte glycoprotein (amino acids 35 to 55) in a total of 200 μl of emulsified incomplete Freund's adjuvant supplemented with 1 mg of *Mycobacterium tuberculosis* (Difco) (complete Freund's adjuvant). Mice received intraperitoneal injections of 200 ng of pertussis toxin (List Biological Laboratories) at the time of immunization and 2 days later. Flow cytometry analysis was performed on cells isolated from indicated organs at day 16 after immunization.

MC38 tumor model

MC38 colon adenocarcinoma cells were cultured in DMEM (Dulbecco's modified essential medium) (10% FBS, 1% penicillin/streptomycin). Mice were inoculated subcutaneously with 5×10^5 MC38 cells in the right flank. Tumor-infiltrating lymphocytes were prepared by mincing and digesting tumor tissues in collagenase IV (1 mg/ml; Roche) and DNase I (200 U ml^{-1}; Sigma-Aldrich) for 1 hour at 37°C, followed by Percoll density gradient centrifugation.

Metabolic assays

Seahorse XF96 extracellular flux analyzer was used to measure OCRs and ECARs under basal conditions and in response to 1 μM oligomycin, 2 μM fluoro-carbonyl cyanide phenylhydrazone (FCCP), and 500 nM rotenone. T_{regs} were activated with anti-CD3 (5 μg ml^{-1}; plate bound), anti-CD28 (5 μg ml^{-1}), and IL-2 (100 U ml^{-1}) for 6 hours before metabolic analysis. Palmitate BSA or BSA control substrate (Agilent) was used where indicated to measure exogenous FAO according to the manufacturer's instructions.

Microarray and GSEA

RNA was extracted with an RNeasy kit (Qiagen) from T_{regs} sorted from WT and *Foxp3*^{Cre}*Myc*$^{fl/fl}$ mice. Microarray analysis was performed, as previously described (*13*). Microarray data from this study have been deposited into the Gene Expression Omnibus (GEO) database with the accession GSE141499. GSEA was performed on publicly available datasets, including neonatal versus adult T_{regs} (GSE66332) (*22*) and activated T_{regs} versus resting T_{regs} from two different datasets [(GSE55753) (*34*); (GSE83315) (*39*)]. eT_{reg} signatures were generated from GSE61077 (*37*).

Statistics

Graphical results (GraphPad Prism software) are presented as means ± SEM with *n* per group and number of experimental replicates indicated in the respective figure legends. Student's *t* test, χ^2 square test, or one-way analysis of variance (ANOVA) with Tukey's multiple comparison test was used where appropriate to generate *P* values. *P* values < 0.05 were considered significant.

SUPPLEMENTARY MATERIALS

Supplementary material for this article is available at http://advances.sciencemag.org/cgi/content/full/6/1/eaaw6443/DC1

Fig. S1. Myc function is important for neonatal T_{reg} function and accumulation.
Fig. S2. Impaired in vitro T_{reg} suppression with Myc deficiency and rescue of immune homeostasis in mixed BM chimeric mice.
Fig. S3. Constitutive Myc expression in T_{regs} does not affect immune homeostasis.
Fig. S4. $CD4^+$ and $CD8^+$ T cell responses in *Foxp3*$^{Cre/DTR}$ mosaic mice and mice with tamoxifen-induced Myc deletion.
Fig. S5. Immune homeostasis in mice with Cox10- or Cpt1a-deficient T_{regs}.

View/request a protocol for this paper from *Bio-protocol*.

REFERENCES AND NOTES

1. S. Z. Josefowicz, L.-F. Lu, A. Y. Rudensky, Regulatory T cells: Mechanisms of differentiation and function. *Annu. Rev. Immunol.* **30**, 531–564 (2012).
2. A. Liston, D. H. D. Gray, Homeostatic control of regulatory T cell diversity. *Nat. Rev. Immunol.* **14**, 154–165 (2014).
3. X. Li, Y. Zheng, Regulatory T cell identity: Formation and maintenance. *Trends Immunol.* **36**, 344–353 (2015).
4. S. Sakaguchi, D. A. A. Vignali, A. Y. Rudensky, R. E. Niec, H. Waldmann, The plasticity and stability of regulatory T cells. *Nat. Rev. Immunol.* **13**, 461–467 (2013).
5. H. Zeng, H. Chi, Metabolic control of regulatory T cell development and function. *Trends Immunol.* **36**, 3–12 (2015).
6. L. A. J. O'Neill, R. J. Kishton, J. Rathmell, A guide to immunometabolism for immunologists. *Nat. Rev. Immunol.* **16**, 553–565 (2016).
7. R. Newton, B. Priyadharshini, L. A. Turka, Immunometabolism of regulatory T cells. *Nat. Immunol.* **17**, 618–625 (2016).
8. M. D. Buck, R. T. Sowell, S. M. Kaech, E. L. Pearce, Metabolic instruction of immunity. *Cell* **169**, 570–586 (2017).
9. R. Wang, C. P. Dillon, L. Z. Shi, S. Milasta, R. Carter, D. Finkelstein, L. L. McCormick, P. Fitzgerald, H. Chi, J. Munger, D. R. Green, The transcription factor myc controls metabolic reprogramming upon T lymphocyte activation. *Immunity* **35**, 871–882 (2011).
10. Z. Nie, G. Hu, G. Wei, K. Cui, A. Yamane, W. Resch, R. Wang, D. R. Green, L. Tessarollo, R. Casellas, K. Zhao, D. Levens, c-Myc is a universal amplifier of expressed genes in lymphocytes and embryonic stem cells. *Cell* **151**, 68–79 (2012).
11. M. Galgani, V. De Rosa, A. La Cava, G. Matarese, Role of metabolism in the immunobiology of regulatory T cells. *J. Immunol.* **197**, 2567–2575 (2016).
12. C. Procaccini, F. Carbone, D. Di Silvestre, F. Brambilla, V. De Rosa, M. Galgani, D. Faicchia, G. Marone, D. Tramontano, M. Corona, C. Alviggi, A. Porcellini, A. La Cava, P. Mauri, G. Matarese, The proteomic landscape of human ex vivo regulatory and conventional T cells reveals specific metabolic requirements. *Immunity* **44**, 406–421 (2016).
13. N. M. Chapman, H. Zeng, T.-L. M. Nguyen, Y. Wang, P. Vogel, Y. Dhungana, X. Liu, G. Neale, J. W. Locasale, H. Chi, mTOR coordinates transcriptional programs and mitochondrial metabolism of activated T_{reg} subsets to protect tissue homeostasis. *Nat. Commun.* **9**, 2095 (2018).
14. R. D. Michalek, V. A. Gerriets, S. R. Jacobs, A. N. Macintyre, N. J. MacIver, E. F. Mason, S. A. Sullivan, A. G. Nichols, J. C. Rathmell, Cutting edge: Distinct glycolytic and lipid oxidative metabolic programs are essential for effector and regulatory $CD4^+$ T cell subsets. *J. Immunol.* **186**, 3299–3303 (2011).
15. V. A. Gerriets, R. J. Kishton, A. G. Nichols, A. N. Macintyre, M. Inoue, O. Ilkayeva, P. S. Winter, X. Liu, B. Priyadharshini, M. E. Slawinska, L. Haeberli, C. Huck, L. A. Turka, K. C. Wood, L. P. Hale, P. A. Smith, M. A. Schneider, N. J. MacIver, J. W. Locasale, C. B. Newgard, M. L. Shinohara, J. C. Rathmell, Metabolic programming and PDHK1 control $CD4^+$ T cell subsets and inflammation. *J. Clin. Invest.* **125**, 194–207 (2015).
16. E. L. Pearce, M. C. Walsh, P. J. Cejas, G. M. Harms, H. Shen, L.-S. Wang, R. G. Jones, Y. Choi, Enhancing CD8 T-cell memory by modulating fatty acid metabolism. *Nature* **460**, 103–107 (2009).
17. A. Angelin, L. Gil-de-Gómez, S. Dahiya, J. Jiao, L. Guo, M. H. Levine, Z. Wang, W. J. Quinn III, P. K. Kopinski, L. Wang, T. Akimova, Y. Liu, T. R. Bhatti, R. Han, B. L. Laskin, J. A. Baur, I. A. Blair, D. C. Wallace, W. W. Hancock, U. H. Beier, Foxp3 reprograms T cell metabolism to function in low-glucose, high-lactate environments. *Cell Metab* **25**, 1282–1293.e7 (2017).
18. V. A. Gerriets, R. J. Kishton, M. O. Johnson, S. Cohen, P. J. Siska, A. G. Nichols, M. O. Warmoes, A. A. de Cubas, N. J. MacIver, J. W. Locasale, L. A. Turka, A. D. Wells, J. C. Rathmell, Foxp3 and Toll-like receptor signaling balance T_{reg} cell anabolic metabolism for suppression. *Nat. Immunol.* **17**, 1459–1466 (2016).
19. B. Raud, D. G. Roy, A. S. Divakaruni, T. N. Tarasenko, R. Franke, E. H. Ma, B. Samborska, W. Y. Hsieh, A. H. Wong, P. Stüve, C. Arnold-Schrauf, M. Guderian, M. Lochner, S. Rampertaap, K. Romito, J. Monsale, M. Brönstrup, S. J. Bensinger, A. N. Murphy, P. J. McGuire, R. G. Jones, T. Sparwasser, L. Berod, Etomoxir actions on regulatory and memory T cells are independent of Cpt1a-mediated fatty acid oxidation. *Cell Metab.* **28**, 504–515.e7 (2018).
20. J. Van den Bossche, G. J. W. van der Windt, Fatty acid oxidation in macrophages and T cells: Time for reassessment? *Cell Metab.* **28**, 538–540 (2018).
21. B. Adkins, C. Leclerc, S. Marshall-Clarke, Neonatal adaptive immunity comes of age. *Nat. Rev. Immunol.* **4**, 553–564 (2004).
22. S. Yang, N. Fujikado, D. Kolodin, C. Benoist, D. Mathis, Regulatory T cells generated early in life play a distinct role in maintaining self-tolerance. *Science* **348**, 589–594 (2015).
23. C.-Y. Huang, A. L. Bredemeyer, L. M. Walker, C. H. Bassing, B. P. Sleckman, Dynamic regulation of *c-Myc* proto-oncogene expression during lymphocyte development revealed by a *GFP-c-Myc* knock-in mouse. *Eur. J. Immunol.* **38**, 342–349 (2008).
24. Y. Y. Wan, R. A. Flavell, Identifying Foxp3-expressing suppressor T cells with a bicistronic reporter. *Proc. Natl. Acad. Sci. U.S.A.* **102**, 5126–5131 (2005).
25. Y. P. Rubtsov, J. P. Rasmussen, E. Y. Chi, J. Fontenot, L. Castelli, X. Ye, P. Treuting, L. Siewe, A. Roers, W. R. Henderson Jr., W. Muller, A. Y. Rudensky, Regulatory T cell-derived interleukin-10 limits inflammation at environmental interfaces. *Immunity* **28**, 546–558 (2008).
26. I. M. de Alboran, R. C. O'Hagan, F. Gärtner, B. Malynn, L. Davidson, R. Rickert, K. Rajewsky, R. A. DePinho, F. W. Alt, Analysis of C-MYC function in normal cells via conditional gene-targeted mutation. *Immunity* **14**, 45–55 (2001).
27. A. Huynh, M. DuPage, B. Priyadharshini, P. T. Sage, J. Quiros, C. M. Borges, N. Townamchai, V. A. Gerriets, J. C. Rathmell, A. H. Sharpe, J. A. Bluestone, L. A. Turka, Control of PI(3) kinase in T_{reg} cells maintains homeostasis and lineage stability. *Nat. Immunol.* **16**, 188–196 (2015).
28. S. Shrestha, K. Yang, C. Guy, P. Vogel, G. Neale, H. Chi, T_{reg} cells require the phosphatase PTEN to restrain T_H1 and T_{FH} cell responses. *Nat. Immunol.* **16**, 178–187 (2015).
29. J. Wei, L. Long, K. Yang, C. Guy, S. Shrestha, Z. Chen, C. Wu, P. Vogel, G. Neale, D. R. Green, H. Chi, Autophagy enforces functional integrity of regulatory T cells by coupling environmental cues and metabolic homeostasis. *Nat. Immunol.* **17**, 277–285 (2016).
30. K. Yang, D. B. Blanco, G. Neale, P. Vogel, J. Avila, C. B. Clish, C. Wu, S. Shrestha, S. Rankin, L. Long, A. KC, H. Chi, Homeostatic control of metabolic and functional fitness of T_{reg} cells by LKB1 signalling. *Nature* **548**, 602–606 (2017).
31. I. Wollenberg, A. Agua-Doce, A. Hernández, C. Almeida, V. G. Oliveira, J. Faro, L. Graca, Regulation of the germinal center reaction by $Foxp3^+$ follicular regulatory T cells. *J. Immunol.* **187**, 4553–4560 (2011).
32. Y. Chung, S. Tanaka, F. Chu, R. I. Nurieva, G. J. Martinez, S. Rawal, Y.-H. Wang, H. Lim, J. M. Reynolds, X.-h. Zhou, H.-m. Fan, Z.-m. Liu, S. S. Neelapu, C. Dong, Follicular regulatory T cells expressing Foxp3 and Bcl-6 suppress germinal center reactions. *Nat. Med.* **17**, 983–988 (2011).
33. M. A. Linterman, W. Pierson, S. K. Lee, A. Kallies, S. Kawamoto, T. F. Rayner, M. Srivastava, D. P. Divekar, L. Beaton, J. J. Hogan, S. Fagarasan, A. Liston, K. G. C. Smith, C. G. Vinuesa, $Foxp3^+$ follicular regulatory T cells control the germinal center response. *Nat. Med.* **17**, 975–982 (2011).
34. A. Arvey, J. van der Veeken, R. M. Samstein, Y. Feng, J. A. Stamatoyannopoulos, A. Y. Rudensky, Inflammation-induced repression of chromatin bound by the transcription factor Foxp3 in regulatory T cells. *Nat. Immunol.* **15**, 580–587 (2014).
35. K. S. Smigiel, E. Richards, S. Srivastava, K. R. Thomas, J. C. Dudda, K. D. Klonowski, D. J. Campbell, CCR7 provides localized access to IL-2 and defines homeostatically distinct regulatory T cell subsets. *J. Exp. Med.* **211**, 121–136 (2014).
36. J. C. Vahl, C. Drees, K. Heger, S. Heink, J. C. Fischer, J. Nedjic, N. Ohkura, H. Morikawa, H. Poeck, S. Schallenberg, D. Rieß, M. Y. Hein, T. Buch, B. Polic, A. Schönle, R. Zeiser, A. Schmitt-Gräff, K. Kretschmer, L. Klein, T. Korn, S. Sakaguchi, M. Schmidt-Supprian, Continuous T cell receptor signals maintain a functional regulatory T cell pool. *Immunity* **41**, 722–736 (2014).
37. A. G. Levine, A. Arvey, W. Jin, A. Y. Rudensky, Continuous requirement for the TCR in regulatory T cell function. *Nat. Immunol.* **15**, 1070–1078 (2014).
38. D. P. Calado, Y. Sasaki, S. A. Godinho, A. Pellerin, K. Köchert, B. P. Sleckman, I. M. de Alborán, M. Janz, S. Rodig, K. Rajewsky, The cell-cycle regulator c-Myc is essential for the formation and maintenance of germinal centers. *Nat. Immunol.* **13**, 1092–1100 (2012).
39. J. van der Veeken, A. J. Gonzalez, H. Cho, A. Arvey, S. Hemmers, C. S. Leslie, A. Y. Rudensky, Memory of inflammation in regulatory T cells. *Cell* **166**, 977–990 (2016).
40. M. DuPage, G. Chopra, J. Quiros, W. L. Rosenthal, M. M. Morar, D. Holohan, R. Zhang, L. Turka, A. Marson, J. A. Bluestone, The chromatin-modifying enzyme Ezh2 is critical for the maintenance of regulatory T cell identity after activation. *Immunity* **42**, 227–238 (2015).
41. D. Zemmour, R. Zilionis, E. Kiner, A. M. Klein, D. Mathis, C. Benoist, Single-cell gene expression reveals a landscape of regulatory T cell phenotypes shaped by the TCR. *Nat. Immunol.* **19**, 291–301 (2018).
42. Y. P. Rubtsov, R. E. Niec, S. Josefowicz, L. Li, J. Darce, D. Mathis, C. Benoist, A. Y. Rudensky, Stability of the regulatory T cell lineage in vivo. *Science* **329**, 1667–1671 (2010).
43. C. T. Luo, W. Liao, S. Dadi, A. Toure, M. O. Li, Graded Foxo1 activity in T_{reg} cells differentiates tumour immunity from spontaneous autoimmunity. *Nature* **529**, 532–536 (2016).

44. S. E. Calvo, K. R. Clauser, V. K. Mootha, MitoCarta2.0: An updated inventory of mammalian mitochondrial proteins. *Nucleic Acids Res.* **44**, D1251–D1257 (2016).
45. H. Y. Tan, K. Yang, Y. Li, T. I. Shaw, Y. Wang, D. B. Blanco, X. Wang, J.-H. Cho, H. Wang, S. Rankin, C. Guy, J. Peng, H. Chi, Integrative proteomics and phosphoproteomics profiling reveals dynamic signaling networks and bioenergetics pathways underlying T cell activation. *Immunity* **46**, 488–503 (2017).
46. S. Schoors, U. Bruning, R. Missiaen, K. C. S. Queiroz, G. Borgers, I. Elia, A. Zecchin, A. R. Cantelmo, S. Christen, J. Goveia, W. Heggermont, L. Goddé, S. Vinckier, P. P. Van Veldhoven, G. Eelen, L. Schoonjans, H. Gerhardt, M. Dewerchin, M. Baes, K. De Bock, B. Ghesquière, S. Y. Lunt, S.-M. Fendt, P. Carmeliet, Fatty acid carbon is essential for dNTP synthesis in endothelial cells. *Nature* **520**, 192–197 (2015).
47. C. V. Dang, *MYC* on the path to cancer. *Cell* **149**, 22–35 (2012).
48. M. E. Brunkow, E. W. Jeffery, K. A. Hjerrild, B. Paeper, L. B. Clark, S.-A. Yasayko, J. E. Wilkinson, D. Galas, S. F. Ziegler, F. Ramsdell, Disruption of a new forkhead/winged-helix protein, scurfin, results in the fatal lymphoproliferative disorder of the scurfy mouse. *Nat. Genet.* **27**, 68–73 (2001).
49. A. Sabò, T. R. Kress, M. Pelizzola, S. de Pretis, M. M. Gorski, A. Tesi, M. J. Morelli, P. Bora, M. Doni, A. Verrecchia, C. Tonelli, G. Fagà, V. Bianchi, A. Ronchi, D. Low, H. Müller, E. Guccione, S. Campaner, B. Amati, Selective transcriptional regulation by Myc in cellular growth control and lymphomagenesis. *Nature* **511**, 488–492 (2014).
50. S. Walz, F. Lorenzin, J. Morton, K. E. Wiese, B. von Eyss, S. Herold, L. Rycak, H. Dumay-Odelot, S. Karim, M. Bartkuhn, F. Roels, T. Wüstefeld, M. Fischer, M. Teichmann, L. Zender, C.-L. Wei, O. Sansom, E. Wolf, M. Eilers, Activation and repression by oncogenic MYC shape tumour-specific gene expression profiles. *Nature* **511**, 483–487 (2014).
51. S. Beer, A. Zetterberg, R. A. Ihrie, R. A. McTaggart, Q. Yang, N. Bradon, C. Arvanitis, L. D. Attardi, S. Feng, B. Ruebner, R. D. Cardiff, D. W. Felsher, Developmental context determines latency of MYC-induced tumorigenesis. *PLOS Biol.* **2**, 1785–1798 (2004).
52. H. Zeng, K. Yang, C. Cloer, G. Neale, P. Vogel, H. Chi, mTORC1 couples immune signals and metabolic programming to establish T_{reg}-cell function. *Nature* **499**, 485–490 (2013).

Acknowledgments: We acknowledge D.R. Green and F.W. Alt for the Myc conditional allele, M. Hendren and A. KC for animal colony management, St. Jude Immunology FACS core facility for cell sorting, and S. A. Lim for help with the EAE animal model. **Funding:** This work was supported by the U.S. NIH (NIH AI105887, AI131703, AI140761, AI150241, AI150514, and CA221290 to H.C.).
Author contributions: J.S. designed, performed, and analyzed experiments and wrote the manuscript. H.Z. designed, performed, and analyzed experiments. Y.D. and G.N. performed bioinformatical analyses. D.B.B., T.-L.M.N., N.M.C., Y.W., S.L., J.L.R., and A.K. performed and analyzed experiments, and N.M.C. and Y.W. edited the manuscript. P.V. provided histopathological analyses. P.C. provided critical reagents and insights. H.C. designed experiments, revised the manuscript, and provided funding and overall direction. **Competing interests:** The authors declare that they have no competing interests. **Data and materials availability:** All data needed to evaluate the conclusions in the paper are present in the paper and/or the Supplementary Materials. Microarray data have been deposited into the GEO database with the accession GSE141499. Additional data related to this paper may be requested from the authors.

Submitted 11 January 2019
Accepted 1 November 2019
Published 1 January 2020
10.1126/sciadv.aaw6443

Citation: J. Saravia, H. Zeng, Y. Dhungana, D. Bastardo Blanco, T.-L. M. Nguyen, N. M. Chapman, Y. Wang, A. Kanneganti, S. Liu, J. L. Raynor, P. Vogel, G. Neale, P. Carmeliet, H. Chi, Homeostasis and transitional activation of regulatory T cells require c-Myc. *Sci. Adv.* **6**, eaaw6443 (2020).